Available online at www.sciencedirect.com
ScienceDirect
Ceramics International 35 (2009) 493–501
CERAMICS INTERNATIONAL
www.elsevier.com/locate/ceramint

Relationship between fracture toughness determined by surface crack in flexure and fracture resistance measured by indentation fracture for silicon nitride ceramics with various microstructures

Hiroyuki Miyazaki *, Hideki Hyuga, Yu-ichi Yoshizawa, Kiyoshi Hirao, Tatsuki Ohji

National Institute of Advanced Industrial Science and Technology (AIST), Anagahora 2266-98, Shimo-shidami, Moriyama-ku, Nagoya 463-8560, Japan

Received 13 November 2007; received in revised form 22 November 2007; accepted 3 January 2008
Available online 8 April 2008

Abstract

The reliability of the Vickers indentation fracture (IF) method for various types of silicon nitride (Si_3N_4) ceramics was assessed by comparing the fracture resistance, K_R obtained from the IF test with the fracture toughness, K_{Ic} from the surface crack in flexure (SCF) technique in the same crack depth region. The K_R of a fine-grained and equiaxed Si_3N_4 matched with the K_{Ic} from the SCF test when Miyoshi's equation was used, while the K_{Ic} of a bearing-grade Si_3N_4 was found to lie between K_R values calculated with Niihara's equation (higher side) and Miyoshi's equations (lower side). In the case of coarse Si_3N_4 with elongated grains, the K_R determined using Niihara's equation gave the best fit with K_{Ic}. The inconsistent outcomes were explained by the probable mechanisms, indicating that the K_R from the IF test cannot be correlated directly with the K_{Ic} unless the effective crack length for the IF test was clarified.

Keywords: C. Toughness and toughening; D. Si_3N_4; Indentation fracture technique

1. Introduction

Silicon nitride (Si_3N_4) is one of the most attractive materials for tribological components since it has superior wear resistance and advantages such as light weight, high strength and toughness, good corrosion resistance and a low thermal expansion coefficient. The drive to replace metal materials with such ceramics for severe and corrosive wear applications has promoted much research to improve the wear resistance and mechanical properties of Si_3N_4 through microstructural control. In particular, Si_3N_4 ball bearings have been developed successively as alternatives to metal materials in the specific circumstances where high rotation speed, low noise, long life and high accuracy are needed [1]. The applications of the developed Si_3N_4 ball bearings have been expanding in many industrial fields, such as hard-disk-bearing spindle motors, high rotation machining tools, devices for semiconductor processes, etc. [1]. For the world-wide market of the Si_3N_4 ball bearings, it is needed to classify the grade of the products by their fracture toughness. However, it is difficult to characterize fracture toughness in such small products from which usual-sized test-bars for single edge-precracked beam (SEPB) [2,3] and surface flaw in flexure (SCF) methods [4] cannot be machined. In such cases, the indentation fracture (IF) technique might be considered as the most suitable technique since it requires only small specimen size and simple experimental procedures [5]. The IF method has also been adopted as the evaluation technique for fracture resistance in the American standard specification for silicon nitride bearing balls [6].

From the theoretical point of view, the fracture resistance, K_R, obtained by the IF technique may differ from the fracture toughness, K_{Ic}, obtained by conventional standard methods such as SEPB or SCF since K_R is for crack arrest, whereas K_{Ic} is for fast crack propagation [7,8]. Thus, the physical basis of estimating K_{Ic} from K_R is strictly not accurate. From an industrial point of view, however, it is desirable that K_{Ic} can be predicted from IF test since both SEPB and SCF techniques are standardized and K_{Ic} determined by these tests is used widely in the engineering field [3,4]. Accordingly, comparisons of K_{Ic} and K_R from the IF method have been conducted by several

* Corresponding author. Tel.: +81 52 736 7486; fax: +81 52 736 7405.
E-mail address: h-miyazaki@aist.go.jp (H. Miyazaki).

0272-8842/$34.00
doi:10.1016/j.ceramint.2008.01.006

researchers and the validity of the estimation of K_{Ic} from K_R has been studied. Ponton and Rawlings evaluated the fracture toughness of 17 different materials including mainly oxide ceramics and glasses and two cermets from the conventional fracture toughness tests such as the single edge notched beam (SENB) test [9]. The resulting toughness values were compared with the indentation fracture resistance obtained from the 19 equations. They showed that there was no universal formula which could be applied to all of these materials. Li et al. determined K_R of a silicon carbide (SiC) ceramic by the IF technique using twelve different equations and compared the results with the K_{Ic} values measured by the conventional fracture toughness tests [10]. They concluded that none of the IF equations yielded reliable fracture resistance values. Quinn and Bradt calculated the K_R of both Si_3N_4 and SiC using three popular IF equations and found that the equation that worked best for Si_3N_4 was not good for SiC [8]. However, there are few systematic studies which evaluated the validity of the IF technique for various kinds of Si_3N_4. Due to the special need to evaluate the fracture resistance of tiny silicon nitride balls, examination of the correlation between K_{Ic} and K_R for different type of Si_3N_4 is necessary.

Our previous study tried to judge the accuracy of IF method using a series of Si_3N_4 ceramics with different microstructures [11]. It was found that the Miyoshi's equation gave the closest value to K_{Ic} from SEPB test for a fine-grained equiaxed Si_3N_4, which was consistent with the previous reports by Awaji et al. [12,13] and Quinn [14]. By contrast, in the case of a sample with coarse microstructure including elongated grains, K_R from Niihara's equation coincided with K_{Ic}, but K_R from Miyoshi's equation was lower than K_{Ic}. However, we could not deny the possibility that the Miyoshi's equation still held effectiveness for the coarse Si_3N_4 as well, since the samples showed rising R-curve behavior and the discrepancy between the K_{Ic} and K_R from Miyoshi's equation might be rationalized by the difference in the measuring point in the R-curve graphs. That is, K_{Ic} from SEPB might represent the toughness value in the long crack region whereas the K_R stood for one in the short-crack region. The difference between K_{Ic} and K_R for the Si_3N_4 with rising R-curve and/or high K_{Ic} has been reported by several researchers [14–16]. Most of them used the above explanation and the reliability of the IF equation has been rarely discussed [15,16]. However, this reason for the differences is speculative since Nose et al. reported that the crack-bridging length in the SEPB specimen of alumina was much smaller than the length of the precrack [2]. There have been few reports that investigate the effective bridging length for SEPB using Si_3N_4. Therefore it seems difficult to evaluate the reliability of the IF method by comparing K_R with K_{Ic} value from SEPB technique unless the effective bridging length for the SEPB specimens is clarified.

In this study, in order to overcome the disadvantages of the SEPB technique, the SCF method as well as SEPB technique, were employed to give reference values, since the crack length can be defined clearly in the SCF test. The indentation fracture resistance, K_R for different types of Si_3N_4 ceramics including ball bearing grade Si_3N_4 were characterized with various indentation loads using four representative equations: Miyoshi et al.'s equation [17] (hereafter Miyoshi's equation) as used in Japanese Industrial Standard (JIS) R 1607 [3], Anstis et al.'s one [18] (hereafter Anstis's equation), Niihara et al.'s one for median cracks [19] (hereafter Niihara's equation) as used in a ceramic ball specification [6] and Ramachandran and Shetty's one [20] (hereafter Ramachandran's equation). The former three formulae are very popular and commonly used. The last equation was selected since its constant was derived theoretically while the Anstis and Niihara equations use adjustable constants obtained by empirical fitting. The ability of four representative IF equations to yield the same K_{Ic} as SCF method was judged in the same crack depth region.

2. Experimental procedure

2.1. Materials

Four kinds of Si_3N_4 ceramics were used in this study. One was a Si_3N_4 for milling balls purchased from the Nikkato Corp. (SUN-12), and two were Si_3N_4 for ball bearings purchased commercially from the Saint-Gobain Ceramics & Plastics Inc. (SN-101C and NBD-200). The final one was prepared by the authors using small amounts of sintering additives. α-Si_3N_4 powder was mixed with 1 wt% Al_2O_3 and 1 wt% Y_2O_3 in ethanol by using nylon-coated iron balls and a nylon pot for 24 h. The slurry was dried, and then passed through 125 mesh. The powders were hot-pressed at 1950 °C for 2 h with an applied pressure of 40 MPa in a 0.9 MPa N_2 atmosphere. Hereafter, we designate this sample as 1A1Y. The density of the sintered bodies was measured using the Archimedes technique. Machined samples were polished and plasma etched in CF_4 gas before microstructural observation by scanning electron microscopy (SEM). The size of the minor axis of each grain was measured in two-dimensional images at magnifications of 10k (1A1Y, SN-101C and NBD200) and 5k (SUN-12). In the high magnification micrographs for the SUN-12 sample, coarse and elongated grains occasionally appeared and most of them were interrupted by the frame of the pictures. In order to capture the whole features of these grains and count their frequency statistically, only coarse grains were selected (major axis $\gtrsim$ 8 μm) from lower magnification micrographs. Median grain diameters were attained from the cumulative distributions (sample size, N, were 1300–1900). Aspect ratios of the grains in the high magnification images were estimated from the mean value of the 10% highest observed aspect ratios [21]. Aspect ratios of the coarse grains selected from the micrographs at lower magnifications were calculated by the same procedure.

2.2. Mechanical test procedure

Young's modulus was measured by the ultrasonic pulse echo method. All the Vickers indentations were made on polished surfaces with a hardness tester (Model AVK-C2, Akashi Corp., Yokohama, Japan). In the case of the 1A1Y sample, indentations were made on the polished surface perpendicular to the hot-pressing axis. The indentation contact time was 15 s. Indentation loads of 19.6, 49, 98, 196, 294 and 490 N were

chosen to vary the crack size over a broad range. Bright field images were observed with a 10× eyepiece and a 50× objective using a traveling microscope (Model MM-40, Nikon Corp., Tokyo, Japan). The lengths of the impression diagonals, $2a$, and surface cracks, $2c$, were measured immediately after the indentation. Only indentations whose four primary cracks emanated straight forward from each corner were accepted. Indentations whose horizontal crack length differed by more than ∼10% from the vertical one were rejected as well as those with badly split cracks or with gross chipping. Eight impressions were made at each load. In most cases, nearly all the indentations were acceptable and the numbers of the indentations, N used for the calculation of K_R at each load was 6–8. When the 1A1Y sample was indented at the load of 490 N, however, some of the indentations experienced serious chipping, which reduced the number to 4. In the case of NBD200 and SUN-12 samples at 19.6 N, $N = 5$ and 3, respectively, because almost half of indentations had unacceptable crack morphology.

For the median–radial crack system, the fracture resistance, K_R, can be determined from the as-indented crack lengths as follows:

$$K_R = \xi\left(\frac{E}{H}\right)^n P c^{-3/2} \quad (1)$$

where ξ is a material-independent constant, n is a dimensionless constant for Vickers-produced radial cracks, E is the Young's modulus, H is the Vickers hardness in the Miyoshi [17], Niihara [19] and Ramachandran [20] equations, whereas it is the mean contact pressure (load over projected area) in the Anstis formula [18]. P is the indentation load and c is the half-length of as-indented surface crack length. H was calculated for each indentation and substituted into Eq. (1) to calculate K_R for each indentation. The values for n in those equations presented by Miyoshi, Anstis and Ramachandran are equal and $n = 1/2$ since these equations were based on the analysis of Lawn et al. [5]. The difference among the three equations lies in the value of ξ: 0.018 for the Miyoshi's equation [17], 0.016 for Anstis's one [18] and 0.023 for Ramachandran's one [20]. In the Niihara's equation [19], $n = 2/5$ and $\xi = 0.0309$.

For fracture toughness measurements, rectangular specimens (4 mm in width × 3 mm in breadth × ∼40 mm in length) were machined from each sintered sample. The SEPB test was performed according to JIS R 1607 with a pop-in crack depth of about 2 mm [3]. For the SCF measurements, the samples were precracked in accordance with the SCF method as described in ISO 18756 [4]. The Knoop indentation loads were 98, 196, 294 and 490 N for SN101C, NBD200 and SUN-12. For 1A1Y sample, indentations were conducted on the surface normal to the hot-pressing direction with the load of 98, 294 and 490 N. The amount of material removed by polishing was 4.5–5 times the depth of the impression for the lower indentation loads, whereas that for loads of 294 and 490 N was 7–8 times the depth of the impression since the lateral cracks became deeper for the indentations with the higher loads. Four-point bending strength was measured with an inner and outer span of 10 and 30 mm, respectively, and a crosshead speed of 0.5 mm/min. Precrack sizes were obtained from SEM micrographs of the fracture surfaces after the test. K_{Ic} was estimated from the crack size, the specimen dimensions, the fracture stress and the stress intensity factor, in accordance with ISO 18756 [4]. The average fracture toughness for each load was calculated from four to six measurements which had acceptable crack morphology.

3. Results

Table 1 shows bulk densities for the four Si_3N_4 materials. The bulk densities were almost the same as the theoretical density of pure β-Si_3N_4 (3.17 g cm^{-3}), indicating that these ceramics were almost fully densified. The variation in the density among the samples may be due to the differences in both the amount and kinds of the sintering additives used for each samples. Fig. 1 shows the microstructures of the samples. It can be seen that 1A1Y sample consists of fine and uniform grains. The size of nearly half of the grains in the SN-101C sample seems nearly same as that in the 1A1Y samples, but the rest of grains are larger (long axis ∼ 2 μm). In the case of NBD200 sample, the selected grains grow further and the rest of the grains remained at similar sizes to those in the 1A1Y sample although the volume fraction of the small grains decreased. The overall grain size becomes apparently larger in the SUN-12 sample and some elongated grains whose long axis was larger than 8 μm were observed. In order to characterize these microstructural features quantitatively, the distributions of grain size for those samples were measured. The results of the grain size analysis are shown in Fig. 2. The sizes of all grains for 1A1Y sample were below 0.9 μm, whereas the maximum grain size for both of the bearing-grade samples were about 1.7 μm, which means that the width of grain size distributions were about two times large than that of 1A1Y. In the case of SUN-12 sample, the distribution curve shifted to the larger grain size side, that is, the fraction of small grains decreased, while that of larger ones increased, leading to the broadest distribution of grain size. Table 1 summarizes median grain diameters and aspect ratios of the four samples. The median grain diameter of SUN-12 was 0.59 μm, which was ∼2.5 times higher than that of 1A1Y (0.24 μm). The aspect ratio of the grains in the high magnification images of the four samples was 4.0–5.6, whereas that of the coarse grains selected from the lower magnification micrographs was ∼10 for SUN-12 samples, indicating that a few of the selected grains had grown unidirectionaly.

Table 1
Bulk density, median grain diameter and aspect ratio of the different kinds of Si_3N_4 ceramics

Property	1A1Y	SN-101C	NBD200	SUN-12
Bulk density (g cm^{-3})	3.19	3.22	3.15	3.20
Median grain diameter (μm)	0.24	0.27	0.40	0.59
Aspect ratio[a]	4.0	5.0	5.6	4.3

[a] Aspect ratio was obtained from the grains in the 5k and 10k magnification images.

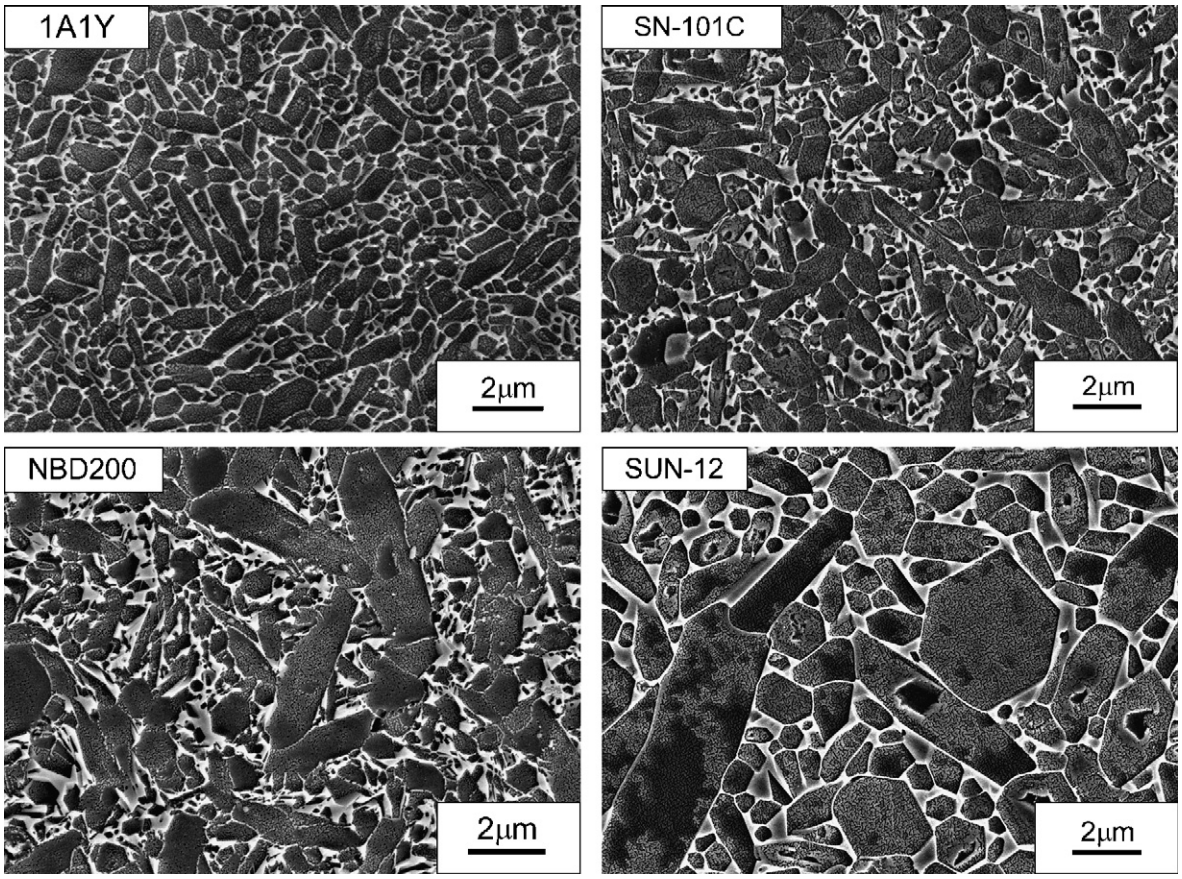

Fig. 1. SEM micrographs of the different kinds of silicon nitride ceramics.

Mechanical properties for the four samples are presented in Table 2. The 1A1Y sample showed the highest Young's modulus and hardness. This was attributed to the quite small volume fraction of grain boundary phases which were softer than pure silicon nitride. By contrast, the fracture toughness of 1A1Y sample measured by the SEPB method was lowest, while that of SUN-12 was highest. By comparing the microstructures of samples and the fracture toughness, it is obvious that the larger the grain grew, the higher the fracture toughness became. The improvement in fracture toughness by coarsening the Si_3N_4 grains is well known [22–24] and is explained by crack bridging of the elongated grains at the crack surface [25,26]. Consequently, it is reasonable to suppose that the bridging mechanism must be at work in the SUN-12 sample but not in the 1A1Y sample.

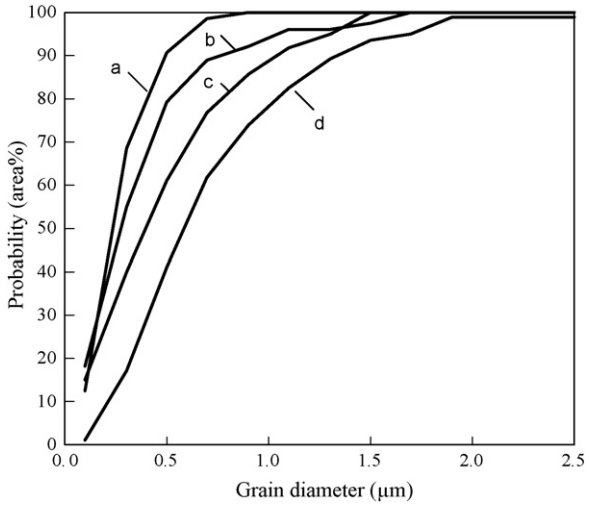

Fig. 2. Distributions of grain diameter for (a) 1A1Y sample, ball bearing-grade silicon nitrides ((b) SN-101C and (c) NBD200) and (d) SUN-12 sample.

Fig. 3 shows a typical profile of a Vickers crack observed with a SEM on the bending specimen fracture surfaces of a SN-101C sample indented at 49 N. The two of dark-gray half-annular contrasts in Fig. 3 demonstrate that the crack was the median–radial (half-penny) type. The crack patterns produced at higher loads exhibited the same median–radial system. Median–radial cracks were also generated in the other samples indented with loads of 49 N and higher. However, the crack

Table 2
Mechanical properties of the different kinds of Si_3N_4 ceramics

Property	1A1Y	SN-101C	NBD200	SUN-12
Young's modulus (GPa)	315	309	314	295
Vickers hardness (GPa)[a]	16.9 ± 0.3	15.7 ± 0.2	15.3 ± 0.3	13.8 ± 0.2
Fracture toughness (MPa $m^{1/2}$)	4.6 ± 0.1	5.9 ± 0.2	5.5 ± 0.1	6.4 ± 0.2

Uncertainties are one standard deviation.
[a] The indentation load was 98 N.

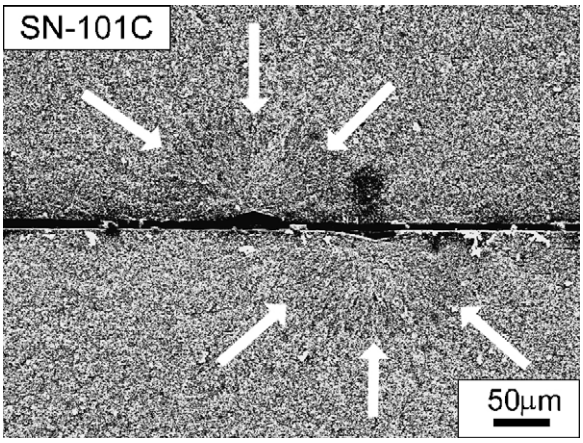

Fig. 3. SEM photo of both fracture halves in a SN-101C sample indented at the load of 49 N.

system for the indentations with the load of 19.6 N could not be identified.

The selected IF equations were described for median–radial crack system and the valid ranges of crack lengths were specified by the ratio of crack length to diagonal size of the "plastic" impression, *c*/*a*. The formulae of Anstis and Ramachandran require $c/a > 2$ [18,20]. Although there is no description of the suitable range of the ratio in Miyoshi's paper, their FEM calculations were based on the empirical data of both *c* and *a* at 196 N and $c/a = 2$ [17]. Therefore a critical value of 2 was also used for the case of the Miyoshi's equation. The Niihara's equation requires *c*/*a* be over ∼2.5 [19]. However, Niihara suggested that the critical ratio of 2.5 for the transition from Palmqvist to the median cracks was worthy of further research [27]. Lube investigated the crack system of silicon nitride ceramics indented at various loads by using the serial sectioning technique and showed that the crack pattern at a load of 98 N was the median–radial type although $c/a = 2.2$ and the pattern at 49 N was median–radial type in some cases regardless of the low *c*/*a* of 1.8 [28]. The Niihara's equation therefore should be also valid for Si_3N_4 whose $c/a < 2.5$ if the crack system was median–radial type. The observed crack patterns of all the indentations at the loads of 49 N and higher were median–radial type as described above, although the ratio of *c*/*a* was between 2.0 and 2.5 for all the indentations at 49 N and those of SN-101C at 98 N. Thus the fracture resistance could be calculated reasonably with Eq. (1) for the indentations at loads of 49 N and higher.

The fracture resistances determined from the as-indented crack lengths are shown in Figs. 4–6, as a function of the indentation load. All four equations showed little dependence on the indentation load for the 1A1Y sample. The fracture resistances calculated with the Niihara's and the Ramachandran's equations were almost the same and were apparently larger than the value from the SPBP method at every indentation load. By contrast, the fracture resistance from

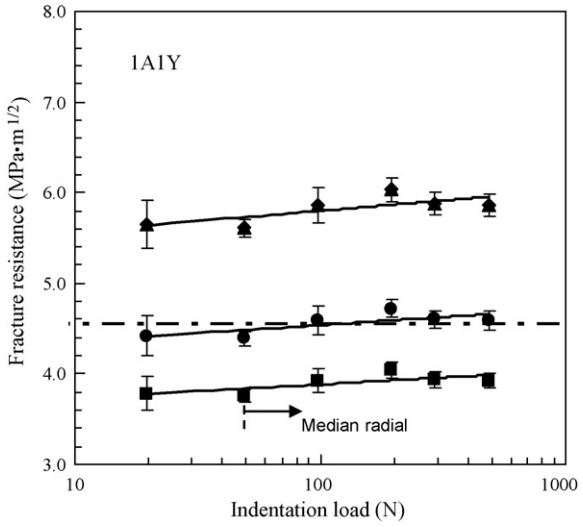

Fig. 4. Dependence of fracture resistance of 1A1Y sample on the indentation loads determined by IF method with equations of Miyoshi (●), Anstis (■), Ramachandran (▲) and Niihara (◆). Dashed and single-dotted line shows fracture toughness from SEPB. Error bars are ±1 standard deviation.

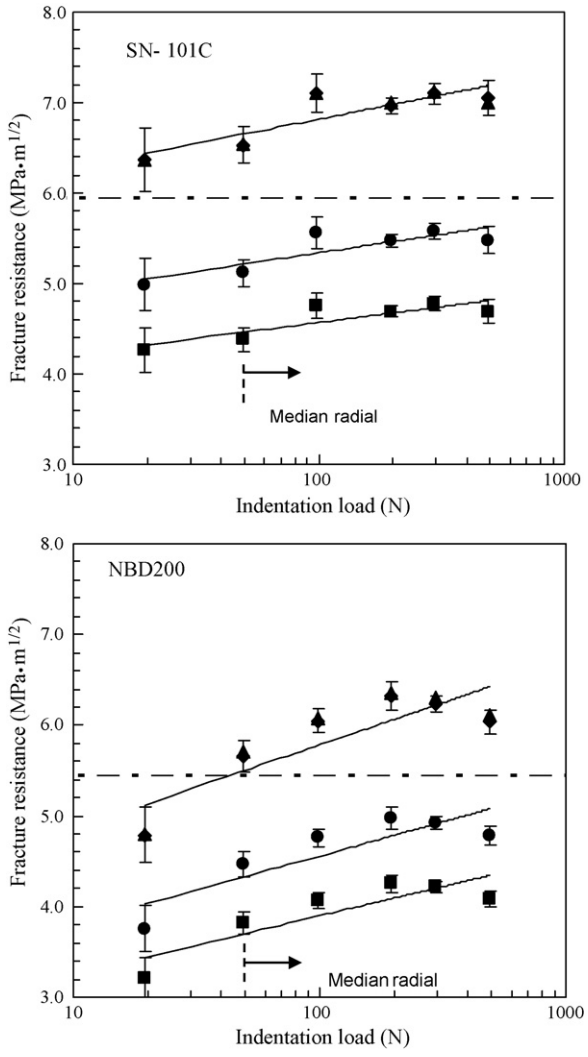

Fig. 5. Dependence of fracture resistance of bearing-grade silicon nitrides (SN-101C and NBD200) on the indentation loads determined by IF method with equations of Miyoshi (●), Anstis (■), Ramachandran (▲) and Niihara (◆). Dashed and single-dotted line shows fracture toughness from SEPB. Error bars are ±1 standard deviation.

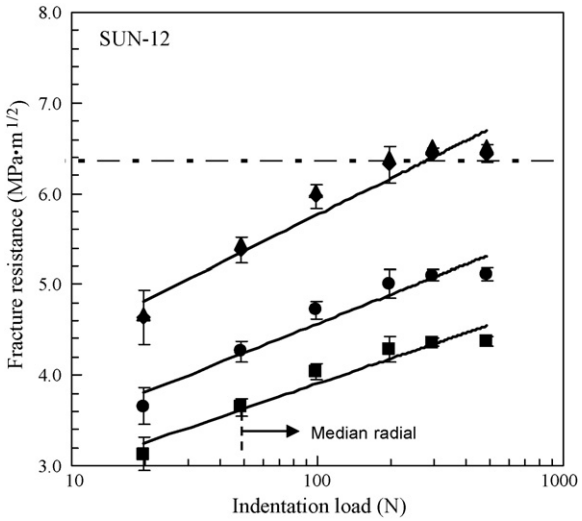

Fig. 6. Dependence of fracture resistance of SUN-12 sample on the indentation loads determined by IF method with equations of Miyoshi (●), Anstis (■), Ramachandran (▲) and Niihara (◆). Dashed and single-dotted line shows fracture toughness from SEPB. Error bars are ±1 standard deviation.

the Anstis's equation showed a smaller value than the fracture toughness from SEPB. K_R from Miyoshi's equation gave the best fit to K_{Ic} from SEPB.

In the case of SN-101C and NBD200 (Fig. 5), the fracture resistances estimated from the Miyoshi and Anstis equations at the low load were far below the fracture toughness from SEPB and increased with the load but did not reach K_{Ic}. K_R from Niihara and Ramachandran equations for the SN-101C sample were higher than K_{Ic} from SEPB. K_R of NBD200 sample from Niihara and Ramachandran equations crossed the K_{Ic} (SEPB) at the load of 49 N. In the case of SUN-12 (Fig. 6), all of the fracture resistances estimated from the four equations exhibited significant dependence on the indentation load, which may indicate the presence of rising *R*-curve behavior for this material. Among the four equations, the estimation with the Niihara and the Ramachandran equations at loads over 196 N gave the closest value to K_{Ic}, while the estimation with the Anstis's and Miyoshi's equation showed much smaller value even at the highest load. All these results are consistent with our previous work which revealed that the best IF equation depends on the microstructure of Si_3N_4 ceramics [11].

It is well known that the increase in fracture resistance with crack extension (rising *R*-curve behavior) in Si_3N_4 is caused by the increment in shielding force which arises from the bridging of elongated grains in the sample [25,26]. Thus, a parameter which represents the bridging length should be used as the *X* axis of a *R*-curve plot when K_R from IF method is compared with K_{Ic} from SCF. As shown in Fig. 3, the damage zones are located at the center of the cracks in the case of IF test, whereas the damage zones were removed in the SCF specimens (Fig. 7). It is reasonable to suppose that the crack depth in the SCF test specimen can be employed as the parameter of the size of crack bridging. However, it is inadequate to use the surface crack length *c*, as a parameter of the crack-bridging length since the bridging should only occur in the crack region excluding the core zone. In this study, crack depth is adopted as the *X* axis of

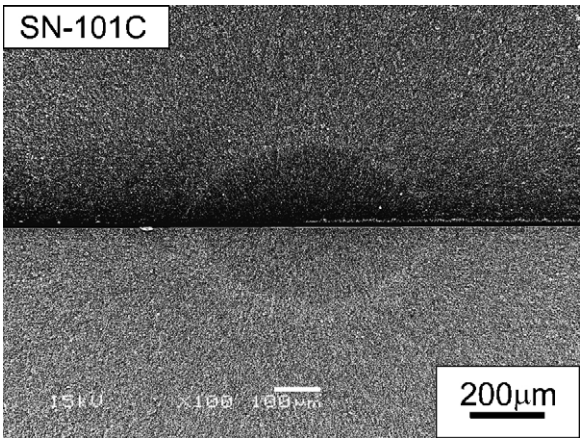

Fig. 7. SEM image of a 294 N precrack in the SN-101C sample.

the *R*-curve plots. The crack depth for the Vickers impression was defined as half the crack length minus half the diagonal size of the plastic impression, $c - a$, because both crack and core zones had half-penny shapes [28].

The K_R from IF technique as a function of crack depth are presented in Figs. 8–10, as well as K_{Ic} from both SCF and SEPB tests. For all samples, K_{Ic} from SCF agreed with the values from SEPB excluding the data of SUN-12 at shorter crack depth, which certified the accuracy of the calculated K_{Ic} values. The crack depth of SCF tests ranged between 100 and 250 μm, which overlapped the range of crack depth of IF tests, which enabled comparison between K_{Ic} and K_R at the same crack depth region as described below. In the case of the 1A1Y sample (Fig. 8), an almost flat *R*-curve was confirmed by the plots of K_R from the four equations, which is attributable to the poor crack bridging as discussed above. The Miyoshi's equation gave the closest outcome to K_{Ic} data from SCF and SEPB. By contrast, the data points of K_R for SN-101C and NBD200 increased with crack depth at short-crack depth

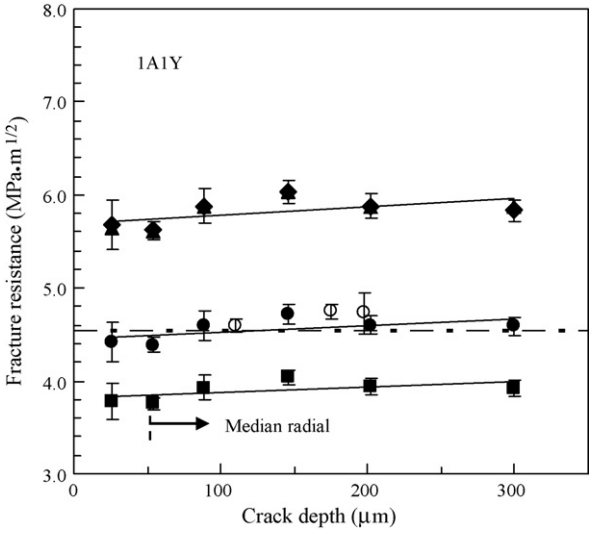

Fig. 8. Fracture resistance versus crack depth for 1A1Y sample determined by IF (closed symbols) and SCF methods (open symbols). (●) Miyoshi, (■) Anstis, (▲) Ramachandran and (◆) Niihara. Dashed and single-dotted line shows fracture toughness from SEPB. Error bars are ±1 standard deviation.

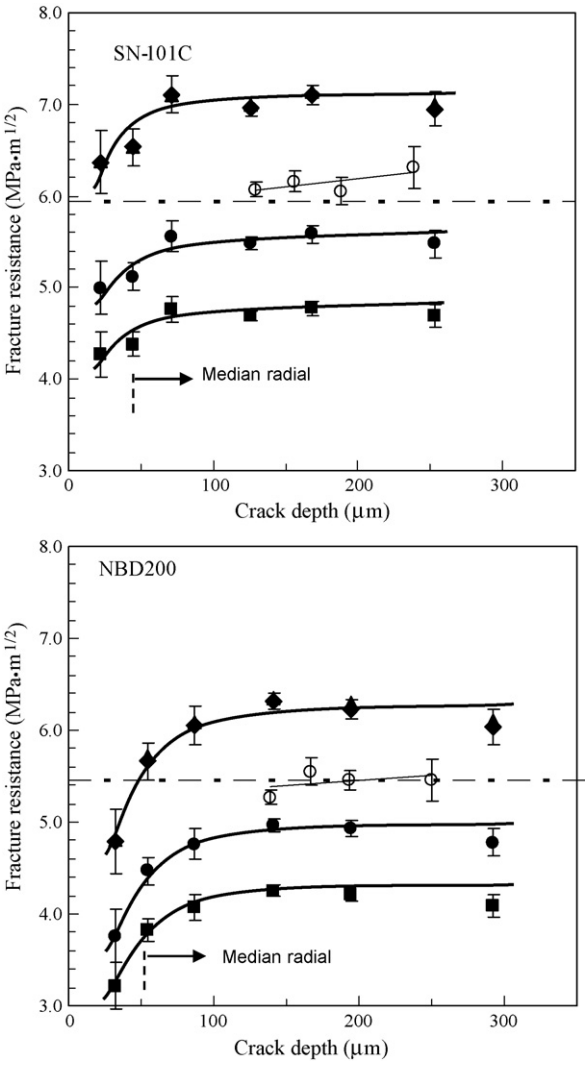

Fig. 9. Fracture resistance versus crack depth for bearing-grade silicon nitrides (SN-101C and NBD200) determined by IF (closed symbols) and SCF methods (open symbols). (●) Miyoshi, (■) Anstis, (▲) Ramachandran and (◆) Niihara. Dashed and single-dotted line shows fracture toughness from SEPB. Error bars are ±1 standard deviation.

(<100 μm), and the slope became smaller in the deeper crack region (Fig. 9). K_R from the Miyoshi's equation was on the lower side of the K_{Ic} and that from Niihara on the upper side. The values were almost equidistant from the K_{Ic} data from SCF. The increase in K_R with the crack depth was more evident for the SUN-12 sample (Fig. 10). K_R from the Niihara and Ramachandran equations at deeper crack regions (>190 μm) matched best with K_{Ic} from SCF. It is obvious from the results that none of the four popular equations could constantly produce matches with the K_{Ic} from SCF.

4. Discussion

Yasuda et al. and Akatsu et al. reported that the SCF method could measure short-crack *R*-curve of Si_3N_4 ceramics and SiC-whisker/Al_2O_3 composites by changing the precrack size by varying the indentation load and/or the amount of material removed after indentation [29,30]. Thus the increase in K_{Ic}

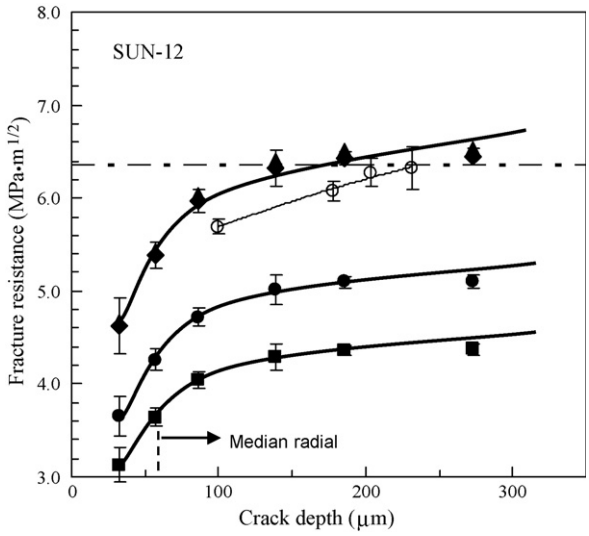

Fig. 10. Fracture resistance versus crack depth for SUN-12 sample determined by IF (closed symbols) and SCF methods (open symbols). (●) Miyoshi, (■) Anstis, (▲) Ramachandran and (◆) Niihara. Dashed and single-dotted line shows fracture toughness from SEPB. Error bars are ±1 standard deviation.

from the SCF for SUN-12 sample with crack depth (Fig. 10) can be regarded as the evidence of the rising *R*-curve of this material, which is consistent with the prediction from the coarse microstructure with elongated grains. It is rational to suppose that the increase in K_R with crack depth for SUN-12 sample reflected the rising *R*-curve behavior.

In the case of the Si_3N_4 consisting of fine and equiaxed grains, some researchers confirmed that the closest outcomes were from the Miyoshi's equation [12–14], which was consistent with our results. The agreement between K_R from the Miyoshi's equation and K_{Ic} from the SCF method is quite reasonable because the constant ξ was derived from the quasi-theoretical analysis of the stress intensity factor using FEM method with the measured values of crack length and diagonal size of Si_3N_4 indented at 196 N [17]. By contrast, the value of ξ for the Ramachandran's equation came from the approximation using the simplified model [20]. It is reasonable to expect that the accuracy of the estimation from such approximation should be inferior to that of Miyoshi's estimation. In the case of the Anstis's and Niihara's equations, the values of ξ were the average using a host of miscellaneous materials such as glasses, Al_2O_3, B_4C and Si_3N_4, etc. [18,19]. The difficulty in detecting the crack tips and the amount of post-indentation slow crack growth differ among these materials [12,13], which would result in the inadequate values of ξ for Si_3N_4 ceramics. Accordingly, in the case of the Si_3N_4, it seems natural that the Miyoshi's equation could produce the nearest values to K_{Ic}.

From the theoretical point of view, only one IF formula should be valid regardless of the difference in microstructures since these formulae were derived from the similar models and share the form but only differ in some adjustable constants. Then, K_R from the Miyoshi's equation should also agree with K_{Ic} in the case of Si_3N_4 with coarse microstructures. One of the possible explanations for the deviation of K_R (Miyoshi) from K_{Ic} can be presented as follows. It was reported that indentation

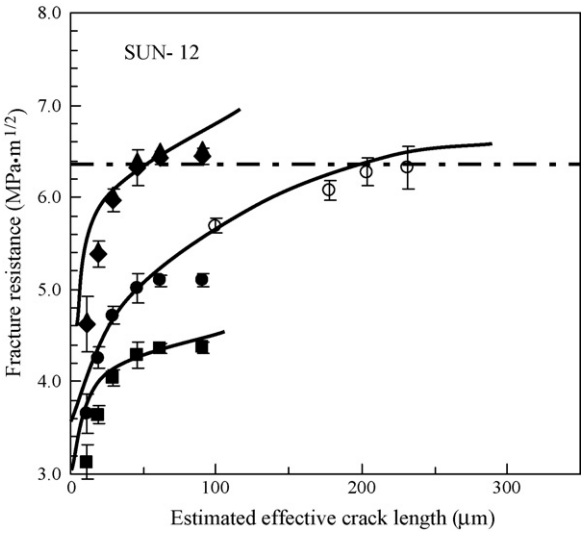

Fig. 11. Fracture resistance versus estimated effective crack length for SUN-12 sample determined by IF (closed symbols) and SCF methods (open symbols). The effective crack lengths for the IF test were estimated as $(c - a)/3$. (●) Miyoshi, (■) Anstis, (▲) Ramachandran and (◆) Niihara. Dashed and single-dotted line shows fracture toughness from SEPB. Error bars are ±1 standard deviation.

cracks in Al_2O_3 exhibited about three times larger crack-opening angle than for long cracks in the standard test method such as single edge-notched bending [31]. Then, the length of crack bridging for the IF test should be much shorter than $c - a$ since the formation of the crack bridging at the large crack opening is difficult. If this is the case, the data points of K_R from the IF test are expected to shift to lower side in X axis. For example, the K_R from IF technique for the SUN-12 sample can be re-plotted against the estimated effective crack length providing that the effective crack lengths for the IF test are $(c - a)/3$ (Fig. 11). In Fig. 11, both K_R from Miyoshi's equation and K_{Ic} from the SCF method are on a same curve. All of the plots for other samples also showed the same good connections between the K_R from Miyoshi's equation and K_{Ic}, indicating that the Miyoshi's equation is best regardless of the difference in microstructures if the assumption is proper. Accordingly, accurate measurements of the real bridging size for the IF test are necessary for further studies to judge the IF equations. Another probable reason is relevant to the crack configuration. Cook et al. reported that the events of lateral cracking affected the constant ξ of the IF equation and its influence depended on the microstructures of alumina ceramics [32]. According to Quinn and Bradt, one of the major reasons for the inconsistent result is that the different types of ceramic materials do not deform and fracture underneath an indentation in a similar manner as many have assumed [8,14]. It is rational to expect that the same phenomena might be operative for various kinds of silicon nitrides, as well. However, it is difficult to conclude that the IF test is unreliable for the various kinds of silicon nitrides since the difference in the bridging size for the IF and SCF tests may be the reason for the discrepancy between K_R and K_{Ic}. Whatever the reasons are, it seems reasonable to conclude that the K_R data obtained by the IF method cannot be used directly at this moment to predict the K_{Ic} for Si_3N_4 with coarse microstructures.

5. Conclusion

Due to the necessity for practical evaluation of fracture resistance, K_R, of small and tough Si_3N_4 samples such as ball bearings, K_R was evaluated by the IF method using the representative formulae for four Si_3N_4 ceramics with different microstructure. The K_R obtained from the four equations was compared to the fracture toughness, K_{Ic}, from the SEPB and SCF methods in the same crack depth region. K_R from the IF method for the Si_3N_4 with fine and uniform microstructure showed little dependence on indentation load and was close to K_{Ic} from the SEPB and SCF tests when the Miyoshi's equation was used. In contrast, K_R of bearing-grade Si_3N_4 ceramics increased with indentation load. K_{Ic} from SCF laid halfway between the data points of Miyoshi's and Niihara's equations. Si_3N_4 ceramics with coarse and elongated grains exhibited a marked rising R-curve and K_R from Niihara and Ramachandran equations matched with K_{Ic} best when the crack depth was larger than 190 μm. Possible reasons for the inconsistent outcomes for the samples with different microstructure were discussed, all of which suggested that there was no straightforward way of correlating the IF method with the SCF method unless the effective size of crack bridging for the IF test was clarified.

Acknowledgment

This work has been supported by METI, Japan, as a part of the international standardization project of test methods for rolling contact fatigue and fracture resistance of ceramics for ball bearings.

References

[1] K. Komeya, Ceram. Trans. 133 (2002) 3–16.
[2] T. Nose, T. Fujii, J. Am. Ceram. Soc. 71 (1988) 328–333.
[3] Testing methods for fracture toughness of fine ceramics, Japanese Industrial Standard, JIS R 1607, 1995.
[4] Fine Ceramics (Advanced Ceramics, Advanced Technical Ceramics)—Determination of Fracture Toughness of Monolithic Ceramics at Room Temperature by the Surface Crack in Flexure (SCF) Method, International Organization for Standards, ISO 18756, Geneva, 2003.
[5] B.R. Lawn, A.G. Evans, B. Marshall, J. Am. Ceram. Soc. 63 (1980) 574–581.
[6] Standard Specification for Silicon Nitride Bearing Balls, ASTM F 2094-03a, 2003.
[7] M. Sakai, R.C. Bradt, Int. Mater. Rev. 38 (1993) 53–78.
[8] G.D. Quinn, R.C. Bradt, J. Am. Ceram. Soc. 90 (2007) 673–680.
[9] C.B. Ponton, R.D. Rawlings, Mater. Sci. Tech. 5 (1989) 961–976.
[10] Z. Li, A. Ghosh, A.S. Kobayashi, R.C. Bradt, J. Am. Ceram. Soc. 72 (1989) 904–911.
[11] H. Miyazaki, H. Hyuga, K. Hirao, T. Ohji, J. Eur. Soc. Ceram. 27 (2007) 2347–2354.
[12] H. Awaji, T. Yamada, H. Okuda, J. Ceram. Soc. Jpn. 99 (1991) 417–422.
[13] H. Awaji, J. Kon, H. Okuda, The VAMAS fracture toughness test round-robin on ceramics, VAMAS Report #9, Japan Fine Ceramic Center, Nagoya, 1990.
[14] G.D. Quinn, Ceram. Eng. Sci. Proc. 27 (2006).
[15] S.R. Choi, J.A. Salem, J. Am. Ceram. Soc. 77 (1994) 1042–1046.

[16] J. Yang, T. Sekino, K. Niihara, J. Mater. Sci. 34 (1999) 5543–5548.
[17] T. Miyoshi, N. Sagawa, T. Sasa, J. Jpn. Soc. Mech. Eng. A 51 (1985) 2489–2497.
[18] G.R. Anstis, P. Chantikul, B.R. Lawn, D.B. Marshall, J. Am. Ceram. Soc. 64 (1981) 533–538.
[19] K. Niihara, R. Morena, D.P.H. Hasselman, J. Mater. Sci. Lett. 1 (1982) 13–16.
[20] N. Ramachandran, D.K. Shetty, J. Am. Ceram. Soc. 74 (1991) 2634–2641.
[21] M. Mitomo, M. Tsutsumi, H. Tanaka, J. Am. Ceram. Soc. 73 (1990) 2441–2445.
[22] E. Tani, S. Umebayashi, K. Kishi, K. Kobayashi, M. Nishijima, Am. Ceram. Soc. Bull. 65 (1986) 1311–1315.
[23] T. Kawashima, H. Okamoto, H. Yamamoto, A. Kitamura, J. Ceram. Soc. Jpn. 99 (1991) 320–323.
[24] N. Hirosaki, Y. Akimune, M. Mitomo, J. Am. Ceram. Soc. 76 (1993) 1892–1894.
[25] P.F. Becher, J. Am. Ceram. Soc. 74 (1991) 255–269.
[26] R.W. Steinbrech, J. Eur. Ceram. Soc. 10 (1992) 131–142.
[27] K. Niihara, R. Morena, D.P.H. Hasselman, J. Am. Ceram. Soc. 65 (1982) C116.
[28] T. Lube, J. Eur. Ceram. Soc. 21 (2001) 211–218.
[29] K. Yasuda, T. Taguchi, J. Tatami, Y. Matsuo, in: M. Matsui, S. Jahanmir, H. Mostaghaci, M. Naito, K. Uematsu, R. Waeshe, R. Morrell (Eds.), Improved Ceramics through New Measurements, Processing and Standards, Ceramic Transaction,, vol. 133, 2002, pp. 115–120.
[30] T. Akatsu, S. Hirai, Y. Tanabe, E. Yasuda, Y. Matsuo, Report of the Research Laboratory of Engineering Materials, vol. 21, Tokyo Institute of Technology, 1996, pp. 55–61.
[31] D. Bleise, R.W. Steinbrech, J. Am. Ceram. Soc. 77 (1994) 315–322.
[32] R.F. Cook, E.G. Liniger, R.W. Steinbrech, F. Deuerler, J. Am. Ceram. Soc. 77 (1994) 303–314.